Splashing morphology and crown dynamics of single droplets impinging heated liquid films

Daniel A. Vasconcelos[1,*], André R. R. Silva[1], Jorge M. M. Barata[1]

1: Universidade da Beira Interior, Covilhã, 6200-001, Portugal
*Corresponding author: daniel.vasconcelos.rodrigues@ubi.pt

Keywords: Droplet impact, Liquid film temperature, Splashing, Crown morphology.

ABSTRACT

The phenomena of droplet impact can be encountered in modern applications, including heat exchangers, electronic cooling devices and internal combustion engines. The underlying mechanisms of two-phase flows, coupled with heat and mass transfer processes, such as evaporation, condensation and boiling, increase the complexity of physical systems. This requires a thorough investigation on interfacial dynamics associated with temperature gradients and mass transfer phenomena. However, existing studies in the literature mainly focus on droplets impacting onto liquid films under ambient conditions, neglecting thermal effects. Therefore, the main objective of this work is to evaluate the influence of the liquid film temperature on the droplet impact outcomes, namely splashing and crown dynamics. An experimental facility was designed and adapted to account for both ambient and non-isothermal conditions. The droplet is released from a hypodermic needle until impacting onto the liquid film. The impact surface is positioned above an aluminium block which acts as a heat source, heating the liquid film by conduction. Water, n-decane and n-heptane are the fluids considered for the experiments. Study cases include varying the droplet impact velocity and liquid film temperature, encompassing both spreading and splashing regimes for isothermal and non-isothermal conditions. Experimental results show that an increase in the liquid film temperature induces the transition from spreading to splashing regimes across all fluids. Qualitatively, this translates from smooth to irregular crowns due to the formation of cusps in the crown rim. These structures are the main source of secondary atomisation, which are promoted by increasing the liquid film temperature. Transitional regimes may display several irregularities, in which splashing is visualised at non-isothermal conditions, followed by the reduction/suppression of the splashing occurrence for higher liquid film temperatures. These require further attention in order to fully comprehend fluid and heat flow, such as Marangoni stresses and local evaporation.

1. Introduction

The droplet impact phenomenon has been extensively researched for a multitude of impact conditions, such as different surfaces (dry, wetted, porous, rough), surrounding environments (cross-flow, droplet wake) and droplet variations (spherical, oscillations, internal circulation) (Rioboo et al., 2001; Josserand et al., 2016; Ferrão et al., 2020; Foltyn et al., 2022). In modern applications, such as heat exchangers, electronic cooling devices and internal combustion engines, temperature plays a major role in the impact dynamics (Selvam et al., 2006; Moreira et al., 2010). For non-isothermal conditions, mass and heat transfer mechanisms arise in the liquid-gas interface, such as evaporation, condensation and boiling. These have been encountered in droplets impacting onto dry heated surfaces, in which the wall temperature exceeds the saturation temperature of the fluid, along with nucleation, Leidenfrost effect, among others (Liang & Mudawar, 2017).

The droplet impact outcomes range from low to high energy impacts, including spreading and coalescence, up to crown and prompt splashing, respectively. Splashing is typically associated with increasing kinetic and thermal effects, leading to more complex topology changes. This is defined by the detachment of secondary droplets from the crown rim. Several authors have investigated this topic regarding influencing parameters on breakup mechanisms. Vander Wal et al. (Vander Wal et al., 2006) explored variable liquid film thicknesses and fluids on the droplet impact phenomenon. Viscosity has an opposite effect for dry and liquid film surfaces, promoting splashing on the dry surface and inhibiting it on wetted surfaces. Higher liquid film thicknesses constrain and inhibit crown and prompt splashing, respectively, as the impact energy dissipates onto the liquid film rather than the developing crown. For increasing surface tension values, the splashing phenomenon is suppressed. Wang and Chen (A.-B. Wang & Chen, 2000) concluded that the critical Weber number is independent of the liquid film thickness for $h^* < 0.1$. Both viscosity and surface tension display a clear influence on ligament breakup and posterior secondary atomisation (Rioboo et al., 2003). The splashing threshold parameter comprises these different variables, characterising the splashing phenomena. The thermophysical properties, inertial properties of the droplet and liquid film, among others, have been evaluated for a variety of impact conditions (Gao & Li, 2015; Okawa et al., 2021; Zhu et al., 2021).

Despite the continuous efforts of the scientific community, impacting droplets onto liquid surfaces are limited to isothermal conditions with the exception of specific applications, such as fire suppression (T. Wang et al., 2021). Therefore, the main objective of this work is to evaluate the influence of the liquid film temperature on droplet impact outcomes, namely splashing and crown dynamics, ranging from ambient conditions to temperatures near the boiling point of the fluid.

2. Experimental Setup

Investigating the droplet impact phenomena requires designing an experimental apparatus to account for both isothermal and non-isothermal conditions. This is divided into several elements, including the heating system, imaging equipment and associated illumination setup, pumping system and impact surface, as displayed by figure 1. The droplet is released from a hypodermic needle through a syringe pump and impacts onto a static liquid film supported by a borossilicate glass surface. This surface is positioned above an aluminium block with 4 embedded cartridge heaters which acts as an heat source. Therefore, the liquid film is affected by a continuous heat flux flowing from the aluminium block to the impact surface. A Photron FASTCAM mini UX50 with a Macro Lens Tokina AT-X M100 AF PRO D was employed with a frame rate and exposure time of $1/4000$ s and $1/25000$ s, respectively, for capturing the impact phenomena. The impact surface is positioned between the high-speed digital camera and an LED lamp combined with a diffusion glass, which provides uniform lighting for optimal image recording. The precision scale is adopted to account for fluid evaporation, as a constant liquid film thickness is required for experiments involving liquid films.

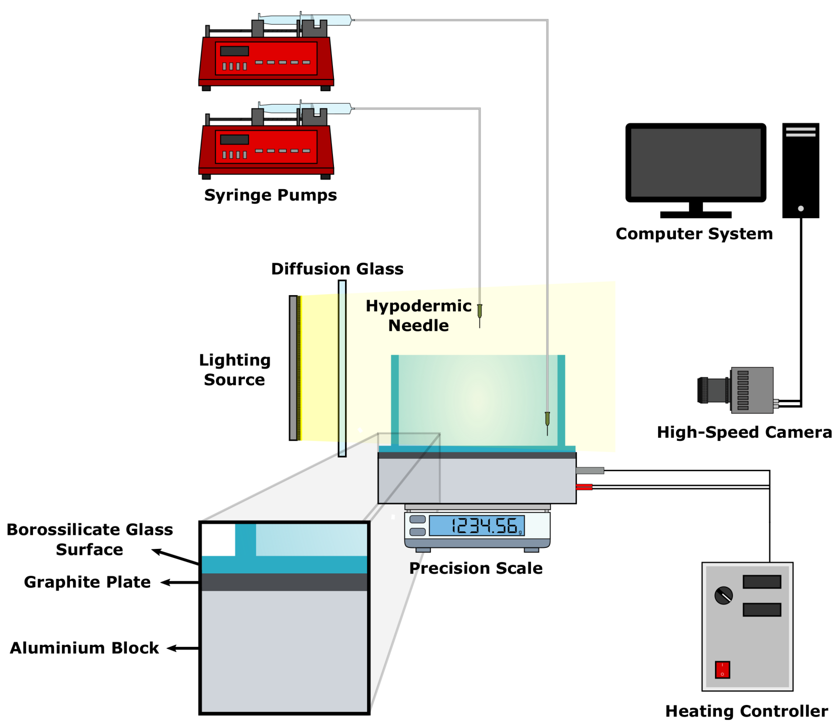

Figure 1. Schematic of the experimental setup (Vasconcelos et al., 2023).

Figure 2 exhibits the schematic of the physical setup. The geometrical parameters associated with this setup are the droplet diameter, D_d, and the liquid film thickness, h. The droplet impinges onto a liquid film with an impact velocity of U_d, which is being heated by a continuous heat flux, q. Due to the temperature differences between the droplet and the liquid film, which leads to a discrepancy in thermophysical properties, a temperature-related variable must be defined. The dimensionless temperature, $\theta = (T_f - T_{air}) / (T_{sat} - T_{air})$, correlates the saturation temperature of the fluid, T_{sat}, the temperature of the liquid film, T_f, and the temperature of the surrounding air, T_{air}. Water, n-decane and n-heptane are the fluids considered for the experiments, as these display significant differences in both saturation temperature and thermophysical properties, which can be visualised in table 1. The experimental methodology consists in heating the liquid film until reaching a specific temperature, followed by guaranteeing a certain liquid film thickness. Once these conditions are met, the droplet is released from the needle until impacting the liquid film. A more detailed description of the experimental setup and methodology is presented in a previous work (Vasconcelos et al., 2023).

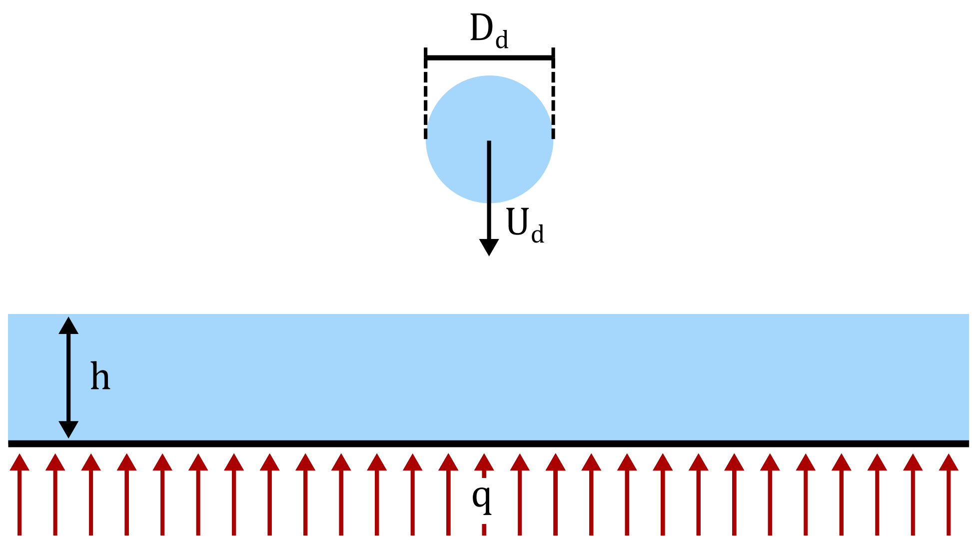

Figure 2. Schematic of a droplet impinging onto a liquid film affected by a heat flux (Vasconcelos et al., 2023).

Fluid	ρ $[\mathrm{kg/m^3}]$	μ $[\mathrm{mPa\,s}]$	σ $[\mathrm{mN/m}]$	T_{sat} $[^\circ\mathrm{C}]$
Water	998.2	1.002	72.73	99.8
N-heptane	685.8	0.412	20.29	98.4
N-decane	732.1	0.929	23.89	174.1

Table 1. Thermophysical properties of water, n-heptane and n-decane at room temperature ($T = 20\ ^\circ\mathrm{C}$) (Vasconcelos et al., 2023).

3. Results and Discussion

Qualitative and quantitative analysis regarding splashing and crown dynamics are performed for a wide range of experimental conditions. The dimensionless numbers for these conditions, namely the Weber and Reynolds number, and the dimensionless liquid film temperature, range from $We = 129$ to $We = 383$, $Re = 2822$ to $Re = 8914$ and $\theta = 0$ to $\theta = 0.8$, respectively, across all fluids. These include non-isothermal and isothermal conditions, as well as both spreading and splashing regimes. The dimensionless liquid film thickness, $h^* = 1.0$, is constant throughout the experiments. Due to the nature of the phenomena, a minimum of 10 droplets are required to ensure a sufficient sample size for evaluating splashing dynamics. The pixel size for the impact phenomena visualisation varies from $27.1\ \mu\mathrm{m}$ to $28.9\ \mu\mathrm{m}$.

Table 2 represents the probability of occurring splashing (p) for a water droplet impacting a heated liquid film. The green color represents splashing, which occurs for a probability of $p > 70\%$, the red color relates to spreading with a probability of $p < 30\%$, and the yellow color is the transition regime ($30\% \leq p \leq 70\%$). For isothermal conditions ($\theta = 0$), an increase in the impact velocity leads to the transition from spreading to splash. These are within the non-splash/splash boundaries defined by Wal et al. (2006). For $\theta > 0$, an increase in the liquid film temperature leads to an increase in the splashing occurrence percentage. This is more visible for experimental conditions close to the transition threshold, such as $U_d = 2.19$ m/s and $U_d = 2.29$ m/s. For these impact velocities, the probability for the occurrence of splashing is equal to 0% for $\theta = 0$ and $\theta = 0.11$, followed by an increase to 38.5% and 90%, respectively. For the outer regions, such as $U_d = 1.88$ m/s and $U_d = 2.71$ m/s, an increase in the liquid film temperature does not alter the outcome of the phenomena. In the transition region, there is a discrepancy which can be visualised for $U_d = 2.29$ m/s and $U_d = 2.42$ m/s for the higher temperatures, which show a slight decrease in the splashing occurrence. This can be visualised in figure 3, which displays the crown formation and splashing for increasing values of liquid film temperature. For $\theta = 0$, the crown displays a smooth rim with no formation of secondary droplets. By increasing the film temperature, for $\theta = 0.23$, several structures arise in the crown rim, which are denominated as fingers. These are usually associated with secondary atomisation, as these ligaments experience stretching and thinning, which may lead to breakup. For $\theta = 0.44$, these structures reach its minimum critical thickness, breaking and forming secondary droplets. The increase in liquid film temperature leading to the regime transition from spreading to splashing is associated with the variation of the thermophysical properties, such as density, surface tension and viscosity. As these decrease with higher temperatures, lower values of viscosity and surface tension promote the occurrence of splashing, as defined by the Weber and Reynolds numbers, as well as the existing non-splash/splashing correlations in the literature. However, for $\theta = 0.6$, the splashing occurrence slightly decreases, as previously mentioned. As displayed by figure 3d, the liquid crown does not display any formation of cusps on the crown rim, as the crown shape is relatively similar to the non-isothermal condition. Due to the transition nature of the experimental conditions, these require further attention in order to fully grasp the impact of temperature on both the thermophysical properties and impact outcome, and to understand these discrepancies that may occur in the transition regime.

Similarly to the previous study, table 3 exhibits the splashing occurrence percentage of n-heptane for different values of impact velocity and dimensionless temperature. For $\theta = 0$, the splash transition occurs for $U_d = 1.52$ m/s. However, in terms of increasing the liquid film temperature, this fluid displays a different behaviour. Despite having close to 100% splashing occurrence for $\theta = 0$ and $\theta = 0.1$ for the transition region ($U_d = 1.52$ m/s and $U_d = 1.68$ m/s), no splashing is verified for $\theta = 0.2$, meaning that, for this region, an increase in the liquid film temperature suppresses the occurrence of splashing. For the lower impact velocity, $U_d = 1.52$ m/s, splashing does not occur until increasing the dimensionless liquid film temperature up to $\theta = 0.81$, whereas for $U_d = 1.68$ m/s,

	Impact velocity [m/s]					
θ	1.88	2.11	2.19	2.29	2.42	2.71
0	0	0	0	0	0	100
0.11	0	0	0	0	0	100
0.23	0	0	38.5	90	10	100
0.44	0	0	90	100	100	100
0.60	0	30	100	80	64	100
0.75	10	10	100	90	80	100

Table 2. Splashing occurrence percentage as a function of the impact velocity and dimensionless temperature for water: - Splashing; - Spreading; - Transition.

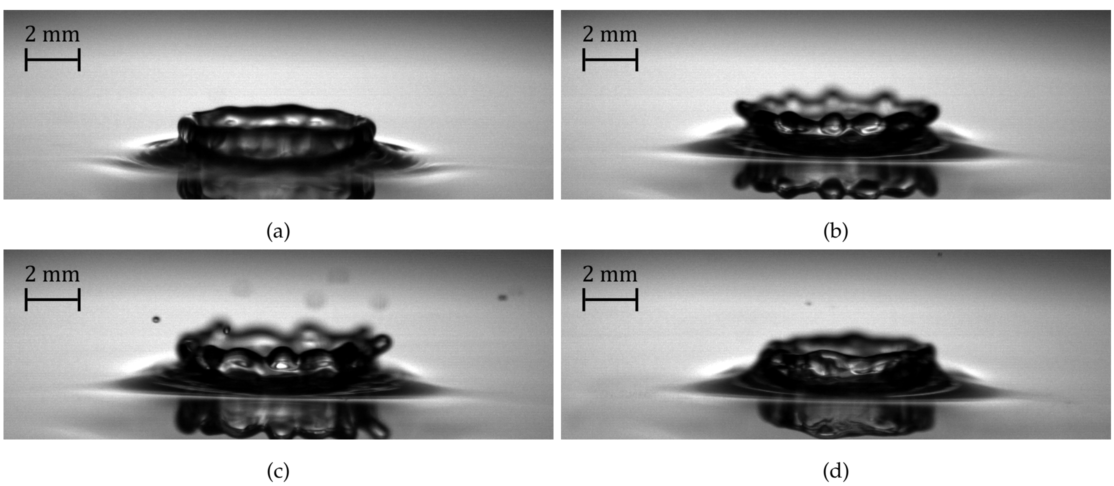

Figure 3. Visualisation of the impact phenomena of a water droplet onto a liquid film for different temperatures $(U_d = 2.42\ \mathrm{m/s},\ D_d = 2.67\ \mathrm{mm})$: a) $\theta = 0$, $\tau = 2.72$; b) $\theta = 0.23$, $\tau = 2.27$; c) $\theta = 0.44$, $\tau = 2.72$; d) $\theta = 0.60$, $\tau = 2.49$.

this transitional field is limited to $\theta = 0.19$ and $\theta = 0.37$, displaying a percentage increase of 0% and 38.5%, respectively. From this point onward, a splashing occurrence of 100% is verified for both impact velocities. These results can be complemented by the impact phenomena visualisation displayed by figure 4. For $\theta = 0$, the crown displays an irregular rim with several detached secondary droplets. For $\theta = 0.19$, however, the splashing phenomenon is suppressed, as the liquid crown displays the formation of fingers, however maintains its shape without leading to breakup. This also occurs for $\theta = 0.37$ which, despite exhibiting more cusps at the free rim and more irregularities, these do not detach from the evolving crown. By significantly increasing the liquid film temperature to $\theta = 0.81$, the developing crown expands, creating instabilities at its rim, which leads to secondary atomisation. This crown displays a more irregular configuration in comparison to lower temperatures. Similarly to water, for impacting droplets onto heated liquid films, there is an indicative of a region, which may be a combination of both thermophysical properties and liquid film temperature, where splashing is reduced or, in the case of n-heptane, suppressed.

	Impact velocity [m/s]				
$\boldsymbol{\theta}$	1.23	1.43	1.52	1.68	2.09
0	0	0	90	100	100
0.1	0	0	80	100	100
0.19	0	10	0	0	100
0.37	0	0	0	38.5	100
0.59	0	10	10	100	100
0.81	0	80	100	100	100

Table 3. Splashing occurrence percentage as a function of the impact velocity and dimensionless temperature for n-heptane: - Splashing; - Spreading; - Transition.

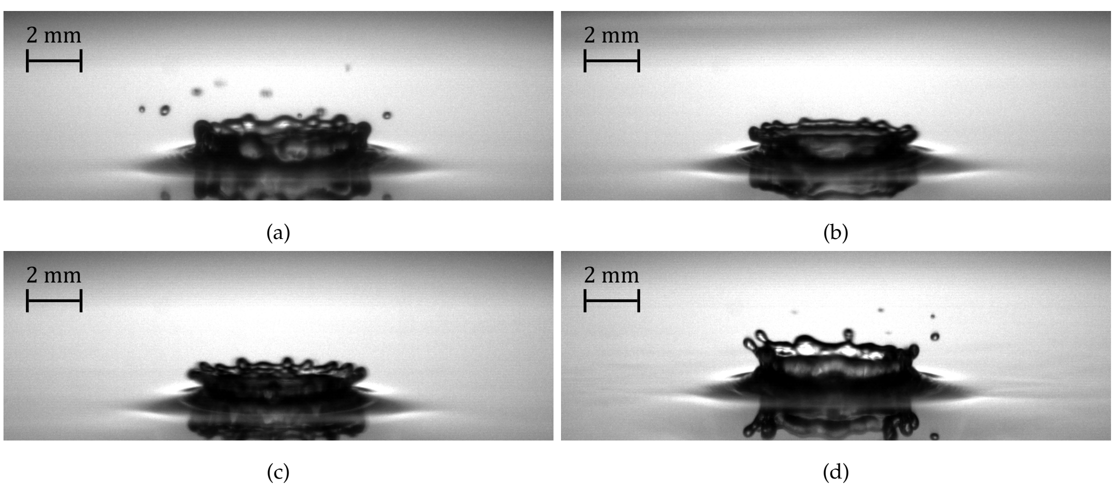

Figure 4. Visualisation of the impact phenomena of an n-heptane droplet onto a liquid film for different temperatures $(U_d = 1.52\ \mathrm{m/s},\ D_d = 2.56\ \mathrm{mm})$: a) $\theta = 0$, $\tau = 1.78$; b) $\theta = 0.19$, $\tau = 1.48$; c) $\theta = 0.37$, $\tau = 1.48$; d) $\theta = 0.81$, $\tau = 1.63$.

N-decane displays similar tendencies to n-heptane, as presented by table 4. The outer regions ($U_d = 1.40$ m/s and $U_d = 2.21$ m/s) are characterised by spreading and splashing, respectively, as the temperature variation does not induce a transition between regimes. For $U_d = 1.65$ m/s and $U_d = 1.72$ m/s, isothermal conditions exhibit a splashing occurrence of $p = 0\%$, corresponding to spreading. This value increases with the dimensionless temperature of the liquid film. For the highest temperature, $\theta = 0.82$, splashing occurs for both impact velocities with an occurrence percentage of $p = 100\%$, whereas $\theta = 0.60$ relates to the transition regime with a splashing occurrence of $p = 60\%$ and $p = 20\%$. These conditions are analogous to the n-heptane droplet impact for $U_d = 1.43$ m/s. For $U_d = 1.80$ m/s and $U_d = 2.05$ m/s, several irregularities can be spotted, similar to the previous fuel. Non-isothermal conditions exhibit splashing, followed by the suppression/reduction of the phenomenon for $\theta = 0.19$, respectively. This is limited to $\theta = 0.19$, as an increase in the liquid film temperature reverts this behaviour, which can be visualised in figure 5. Opposite to n-heptane, the crown rims are relatively homogeneous in terms of shape and formation of cusps for the different dimensionless temperatures. Lower temperatures, $\theta = 0$ and $\theta = 0.1$, are characterised by secondary droplets which mostly originate from prompt splashing at earlier stages of the impact. The phenomenon is suppressed for $\theta = 0.2$, as previously mentioned, and the breakup dynamics reappear for higher temperatures. Qualitatively, the secondary droplets at higher temperatures exhibit greater sizes in comparison to lower temperatures.

	Impact velocity [m/s]					
$\boldsymbol{\theta}$	1.40	1.65	1.72	1.80	2.05	2.21
0	0	0	0	100	100	100
0.10	0	0	0	80	100	90
0.19	0	0	0	10	60	100
0.42	0	10	10	100	100	100
0.60	0	60	20	100	100	100
0.82	0	100	100	100	100	100

Table 4. Splashing occurrence percentage as a function of the impact velocity and dimensionless temperature for n-decane: - Splashing; - Spreading; - Transition.

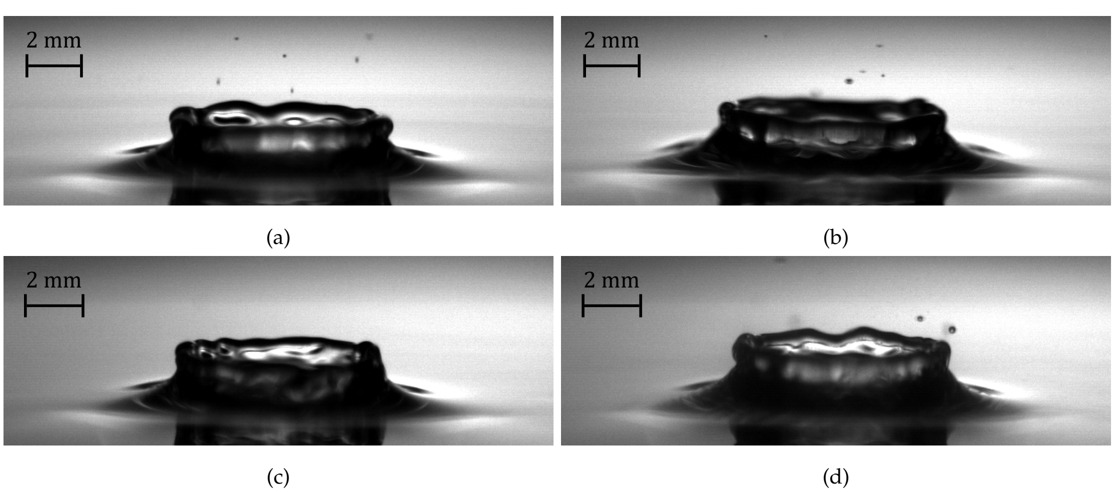

Figure 5. Visualisation of the impact phenomena of an n-decane droplet onto a liquid film for different temperatures $(U_d = 1.80 \text{ m/s},\ D_d = 2.72 \text{ mm})$: a) $\theta = 0$, $\tau = 6.62$; b) $\theta = 0.10$, $\tau = 7.94$; c) $\theta = 0.19$, $\tau = 5.96$; d) $\theta = 0.37$, $\tau = 6.62$.

Overall, the liquid film temperature is a defining factor in altering the impact outcome, such as secondary atomisation and crown development. This is due to several aspects, such as the variation of the thermophysical properties, as higher temperatures lead to lower values of density, viscosity and surface tension. However, transitional regimes, where the splashing occurrence fluctuates, require additional studies. These include both heated droplet and liquid film, different fluids, among others, which may give insight onto non-isothermal conditions. The non-splash/splash boundaries should also be adapted to account for temperature differences.

4. Conclusions

The crown and splashing dynamics were evaluated qualitative and quantitatively as a function of the impact velocity and dimensionless temperatures. The droplet impact phenomena at isothermal conditions are in agreement with experimental data reported in the literature. An increase in the liquid film temperature leads to a regime transition from spreading to splashing across all fluids. This is verified in terms of crown development, as it promotes the formation of cusps in the crown rim, possibly leading to breakup and posterior secondary atomisation. Transitional regimes may display several irregularities, such as splashing suppression/reduction, which is the case for fuels at $\theta = 0.2$ and water at $\theta = 0.6$, respectively.

Acknowledgements

The present work was performed under the scope of Aeronautics and Astronautics Research Center (AEROG) of the Laboratório Associado em Energia, Transportes e Aeronáutica (LAETA) activities, supported by Fundação para a Ciência e Tecnologia (FCT) through the projects number UIDB/50022/2020, UIDP/50022/2020 and LA/P/0079/2020, and by the Ph.D. scholarship with the reference SFRH BD/143307/2019.

Nomenclature

D_d	Droplet diameter $[\mathrm{m}]$
h	Liquid film thickness $[\mathrm{m}]$
h^*	Dimensionless liquid film thickness $[-]$
p	Splashing occurrence probability $[-]$
q	Heat flux $[\mathrm{W/m^2}]$
Re	Reynolds number $[-]$
T_{sat}	Saturation temperature $[\mathrm{K}]$
U_d	Impact velocity $[\mathrm{m/s}]$
We	Weber number $[-]$
θ	Dimensionless Temperature $[-]$

μ Viscosity $[\mathrm{kg}/(\mathrm{m} \cdot \mathrm{s})]$
ρ Density $\left[\mathrm{kg}/\mathrm{m}^3\right]$
σ Surface tension $\left[\mathrm{kg} \cdot \mathrm{m}^2/\mathrm{s}^2\right]$
τ Dimensionless time $[-]$

References

Ferrão, I., Vasconcelos, D., Ribeiro, D., Silva, A., & Barata, J. (2020). A study of droplet deformation: The effect of crossflow velocity on jet fuel and biofuel droplets impinging onto a dry smooth surface. *Fuel*, *279*, 118321.

Foltyn, P., Ribeiro, D., Silva, A., Lamanna, G., & Weigand, B. (2022). Influence of wetting behavior on the morphology of droplet impacts onto dry-patterned micro-structured surfaces. *Physics of Fluids*, *34*(12).

Gao, X., & Li, R. (2015). Impact of a single drop on a flowing liquid film. *Physical Review E*, *92*(5), 053005.

Josserand, C., Ray, P., & Zaleski, S. (2016). Droplet impact on a thin liquid film: anatomy of the splash. *Journal of Fluid Mechanics*, *802*, 775–805.

Liang, G., & Mudawar, I. (2017). Review of drop impact on heated walls. *International Journal of Heat and Mass Transfer*, *106*, 103–126.

Moreira, A., Moita, A., & Panao, M. (2010). Advances and challenges in explaining fuel spray impingement: How much of single droplet impact research is useful? *Progress in energy and combustion science*, *36*(5), 554–580.

Okawa, T., Kubo, K., Kawai, K., & Kitabayashi, S. (2021). Experiments on splashing thresholds during single-drop impact onto a quiescent liquid film. *Experimental Thermal and Fluid Science*, *121*, 110279.

Rioboo, R., Bauthier, C., Conti, J., Voue, M., & De Coninck, J. (2003). Experimental investigation of splash and crown formation during single drop impact on wetted surfaces. *Experiments in fluids*, *35*, 648–652.

Rioboo, R., Tropea, C., & Marengo, M. (2001). Outcomes from a drop impact on solid surfaces. *Atomization and sprays*, *11*(2).

Selvam, R. P., Lin, L., & Ponnappan, R. (2006). Direct simulation of spray cooling: Effect of vapor bubble growth and liquid droplet impact on heat transfer. *International Journal of Heat and Mass Transfer*, *49*(23-24), 4265–4278.

Vander Wal, R. L., Berger, G. M., & Mozes, S. D. (2006). Droplets splashing upon films of the same fluid of various depths. *Experiments in fluids*, *40*(1), 33–52.

Vasconcelos, D. A., Silva, A. R., & Barata, J. M. (2023). The impact of temperature on heated liquid films: Crater and jetting impact dynamics. *Experimental Thermal and Fluid Science*, *147*, 110944.

Wal, R. L. V., Berger, G. M., & Mozes, S. D. (2006). The splash/non-splash boundary upon a dry surface and thin fluid film. *Experiments in fluids*, *40*(1), 53–59.

Wang, A.-B., & Chen, C.-C. (2000). Splashing impact of a single drop onto very thin liquid films. *Physics of fluids*, *12*(9), 2155–2158.

Wang, T., Wang, C., Rui, S., & Pan, K. (2021). Effect of the liquid temperature on the interaction behavior for single water droplet impacting on the immiscible liquid. *Chinese Physics B*, *30*(11), 116801.

Zhu, J., Tu, C., Lu, T., Luo, Y., Zhang, K., & Chen, X. (2021). Behavior of a water droplet impacting a thin water film. *Experiments in Fluids*, *62*, 1–13.